mathematics

Article

Hybrid Attitude Saturation and Fault-Tolerant Control for Rigid Spacecraft without Unwinding

Jun Ma , Zeng Wang * and Chang Wang

Xi'an Key Laboratory of Intelligence, Xi'an Technological University, Xi'an 710021, China; majun@xatu.edu.cn (J.M.); wangchang86@st.xatu.edu.cn (C.W.)
* Correspondence: wangzeng@xatu.edu.cn

Abstract: This paper tackles the saturation and fault-tolerant attitude tracking problem without unwinding for rigid spacecraft with external disturbances and partial loss of actuator effectiveness faults. A hybrid saturation and fault-tolerant attitude control (HSFC) is proposed. The Lyapunov method is employed to prove that the tracking errors of the spacecraft system tend to the equilibrium point asymptotically with HSFC. The advantages of the HSFC are that it is fault-tolerant, anti-unwinding and explicitly upper bounded a priori which means that both actuator saturation and the unwinding phenomenon can be avoided. Simulations verify the effectiveness of the proposed approach.

Keywords: spacecraft attitude control; saturation control; unwinding; fault tolerant

MSC: 93D20

check for updates

Citation: Ma, J.; Wang, Z.; Wang, C. Hybrid Attitude Saturation and Fault-Tolerant Control for Rigid Spacecraft without Unwinding. *Mathematics* **2023**, *11*, 3431. https://doi.org/10.3390/math11153431

Academic Editors: Haizhao Liang, Jianying Wang and Chuang Liu

Received: 17 July 2023
Revised: 2 August 2023
Accepted: 3 August 2023
Published: 7 August 2023

1. Introduction

In the last few decades, the attitude control of rigid spacecraft has attracted extensive attention and several elegant attitude control strategies for rigid spacecraft have been proposed. More specifically, the authors of [1] using the passivity theory develop an adaptive control scheme for the attitude control of rigid spacecraft. In [2], an adaptive finite time non-singular terminal sliding mode attitude tracking control (AFNTSMC) scheme is presented for uncertain rigid spacecraft. In [3], the authors propose a simple non-singular terminal sliding mode control (NTSMC) to obtain high precision and robust finite-time bounded attitude tracking for rigid spacecraft with finite-time stability. In [4], a new integral sliding mode control integrating the bi-limit homogeneous theory is explored to obtain fixed-time stability for rigid spacecraft attitude tracking. Recently, the authors of [5] exploit the predefined-time guaranteed performance takeover control for non-cooperative spacecraft.

But, these aforementioned controls are formulated with the assumption that the actuators could supply any requested torque for the attitude control of spacecraft. In a practical scenario, when the requested control torque exceeds the maximum value that the actuator can supply, the performance of the spacecraft system cannot be guaranteed and even leads to instability. Obviously, it is more unrealistic to design a robust control strategy under the above assumption [6,7]. Recognizing this drawback, several approximate solutions that take into account actuator constraints have been proposed. Particularly, the authors of [8] propose a continuous globally robust attitude saturation control for spacecraft in the presence of parametric uncertainty and external disturbances. In [9], a nonlinear backstepping attitude saturation control integrating the inverse tangent-based tracking function and a family of augmented Lyapunov functions is exploited to achieve attitude maneuver of rigid spacecraft. In [10], an adaptive saturation attitude tracking control is designed for rigid spacecraft with unknown system parameters and disturbance. In [11], two very simple saturated PD (SPD) controllers are developed for rigid spacecraft to obtain global asymptotic stabilization. Subsequently, velocity-free asymptotic attitude stabilization control is introduced for rigid spacecraft in the presence of actuator constraints [12]. In [13], a unified formulation of simple but effective SPD control is proposed for asymptotic stabilization of spacecraft in the presence of actuator constraints. In [14], a simple single saturated PD (SSPD) control is proposed for spacecraft stabilization. In [15], a saturated output feedback finite-time proportional–derivative control is developed for spacecraft subject to actuator constraints and attitude measurements only.

In spite of the above-mentioned schemes addressing the attitude saturation problem of the spacecraft, they do not consider the actuator faults. It should be pointed out that actuator faults of spacecraft may dramatically degrade the attitude tracking performance [16,17]. To eliminate this weakness, a fault-tolerant technique is added to the spacecraft attitude control scheme to improve the safety and accuracy of the attitude tracking. Recognizing this benefit, several effective fault-tolerant control schemes for spacecraft attitude control have been developed to compensate actuator failure. The authors of [18] develop an adaptive robust fault-tolerant control to tackle the spacecraft attitude tracking problem. In [19], an adaptive fault-tolerant control with fast transient is proposed to address spacecraft attitude tracking. The authors of [20] introduce a fault-tolerant on-line control to solve the spacecraft attitude tracking with actuator failure. In [21], a fixed-time fault-tolerant attitude tracking control is explored for rigid spacecraft described by the unit quaternion subject to model uncertainties, external disturbances and actuator faults. In [22], based on the fixed-time disturbance observer, a quantized fixed-time control is introduced to obtain attitude stabilization. In [23], an incremental nonlinear control technology is used to simplify the attitude control system with a synthetic uncertainty or fault term.

For the unit-quaternion representation, although it is a global nonsingularity, it has the weakness of the unwinding phenomenon [24]. In comparison with the almost 'global' stability in the above quaternion-based controls, the hysteresis-based hybrid attitude control can ensure that the global stability of the spacecraft system is obtained. Recognizing these advantages, several hysteresis-based hybrid attitude control schemes have been exploited. The authors of [25] propose a quaternion-based hybrid feedback scheme to address global attitude stabilization without the angular velocity measurement. The authors of [26] present a smooth control system, which can provide almost semi-global exponential stability. The authors of [27] introduce a hybrid certainty equivalence controller scheme with a hybrid observer for the rigid spacecraft with only quaternion measurement. More recently, in [28], a global finite-time attitude control based on the hybrid control technique is designed to solve the attitude tracking of a rigid body using a quaternion description. In [29], a saturated hybrid output feedback PD plus (SHOPD+) scheme with attitude measurements only is developed to achieve global stability for rigid spacecraft subject to the actuator limit. Furthermore, a velocity-free saturated hybrid proportional–derivative (PD) plus (PD+) control is constructed to achieve global finite-time attitude tracking for spacecraft [30]. The authors of [31] present a novel anti-unwinding finite-time attitude tracking control law with a designed control signal which works within a known actuator-magnitude constraint using a continuous nonsingular fast terminal sliding mode (NFTSM) concept.

In this paper, a simple hybrid attitude saturation and fault-tolerant control is proposed to address the spacecraft attitude tracking problem subject to external disturbances and partial loss of actuator effectiveness faults. An adaptive hybrid robust saturation control is developed to obtain global stability which means the tracking errors tend to the equilibrium point asymptotically without the unwinding phenomenon. In comparison with the existing saturation attitude controls of spacecraft in [29,30], the proposed control can tackle actuator faults. Compared with the available fault-tolerant control schemes for spacecraft in [31], the proposed control can remove the possibility of degraded or unpredictable motion and actuator failure due to excessive torque input levels by selecting control gains a priori. Advantages of the proposed control include anti-unwinding, global stability, control constraint, fault-tolerance and robustness. Simulations are performed on the spacecraft to verify the effectiveness performance of the developed HSFC.

Throughout this paper, notations $\lambda_m(K)$ and $\lambda_M(K)$ are utilized to denote the smallest and largest eigenvalues, respectively, of a symmetric positive-definite bounded matrix K.

We use $\|x\| = \sqrt{x^T x}$ to define the norm of a vector $x \in R^n$ and the corresponding induced norm $\|K\| = \sqrt{\lambda_M(K^T K)}$ is used to define the norm of a matrix K, and I_3 denotes an $R^{3\times 3}$ identity matrix.

The framework of this paper is organized as follows. The preliminaries are given in Section 2. The control design including hybrid system and controller formulation is presented in Section 3. In Section 4, asymptotic stability analysis is given. In Section 5, numerical simulations are illustrated to verify the effectiveness performance of the proposed approach. Finally, the conclusion is presented in Section 6.

2. Preliminaries

2.1. Spacecraft Model and Properties

The attitude kinematics and dynamics of a rigid spacecraft are formulated as [2,32]:

$$\begin{cases} \dot{q}_v = \frac{1}{2}(q_4 I_3 + q_v^{\times})\omega, \\ \dot{q}_4 = -\frac{1}{2} q_v^T \omega. \end{cases} \tag{1}$$

$$J\dot{\omega} = -\omega^{\times} J\omega + u + d. \tag{2}$$

where a unit quaternion $q \in \bar{S}^3 = \left\{x \in R^4 : x^T x = 1\right\}$ is used to describe the attitude orientation of the spacecraft in the body frame with respect to an inertial frame, and $\bar{S}^3$ denotes the three-dimensional sphere embedded in R^4, $q = (q_v, q_4)$ includes vector $q_v \in R^3$ and scalar $q_4 \in R$ and satisfies the constraint $q_v^T q_v + q_4^2 = 1$, $\omega \in R^3$ represents the angular velocity, $J \in R^{3\times 3}$ denotes the constant symmetric positive-definite inertia matrix of the spacecraft, $u = [u_{\tau 1}, u_{\tau 2}, u_{\tau 3}]^T \in R^3$ denotes the control torque, $d \in R^3$ represents the external disturbances, and the operation $(\cdot)^{\times} \in R^{3\times 3}$ denotes a skew-symmetric matrix, that is

$$z^{\times} = \begin{bmatrix} 0 & -z_3 & z_2 \\ z_3 & 0 & -z_1 \\ -z_2 & z_1 & 0 \end{bmatrix}, \quad \forall z = [z_1, z_2, z_3] \in R^3. \tag{3}$$

Assumption 1 ([21,23]). *The desired angular velocity ω_d and its first derivative are bounded by $\|\omega_d\| \le c_1$ and $\|\dot{\omega}_d\| \le c_2$, respectively, where c_1 and c_2 are known positive constants.*

Assumption 2 ([8,33]). *Assume that the disturbance d is bounded by $\|d\| \le l_g$ where l_g is a known positive constant.*

Assumption 3 ([29]). *The inertia matrix J is bounded by $\|J\| \le J_M$, where J_M is a known positive constant.*

Property 1 ([29]). *The following properties hold for the skew-symmetric matrices $a^{\times}$ and $b^{\times}$ with $a, b \in R^3$*

$$a^{\times} b^{\times} = b a^T - a^T b I_3. \tag{4}$$

$$a^{\times} b = -b^{\times} a. \tag{5}$$

$$\|a^{\times}\| = \|a\|. \tag{6}$$

Property 2 ([29]). *The matrix $(C\omega_d)^{\times} J + J(C\omega_d)^{\times}$ is skew-symmetric matrix and C is the rotation matrix.*

2.2. Problem Statement

The desired attitude $q_d = (q_{dv}^T, q_{d4})^T \in R^3 \times R$ is defined by [8,32]

$$\begin{cases} \dot{q}_{dv} = \frac{1}{2}(q_{d4} I_3 + q_{dv}^{\times})\omega_d, \\ \dot{q}_{d4} = -\frac{1}{2} q_{dv}^T \omega_d. \end{cases} \tag{7}$$

The relative attitude tracking error of the spacecraft is defined by $q_e = (e_v^T, e_4)^T \in \bar{S}^3$ where $e_v = [e_1, e_2, e_3] \in R^3$ and $e_4 \in R$. Then, the attitude tracking problem can be described as follows.

$$\begin{cases} \dot{e}_v = \frac{1}{2}(e_4 I_3 + e_v^{\times})\omega_e, \\ \dot{e}_4 = -\frac{1}{2} e_v^T \omega_e. \end{cases} \tag{8}$$

$$J\dot{\omega}_e = -\omega^{\times} J\omega + J\left(\omega_e^{\times} C\omega_d - C\dot{\omega}_d\right) + \Gamma u + d. \tag{9}$$

$$\omega_e = \omega - C\omega_d. \tag{10}$$

where the diagonal matrix $\Gamma = diag(\gamma_1(t),\ \gamma_2(t),\ \gamma_3(t)) \in R^{3\times 3}$ denotes the actuator health condition and $\gamma_i(t)$ satisfies $\gamma_0 \le \gamma_i(t) \le 1,\ (i = 1,2,3)$ with a known positive constant γ_0. Clearly, $\gamma_i(t) = 1$ indicates the fault-free spacecraft and $\gamma_0 \le \gamma_i(t) \le 1$ denotes that the ith actuator partially loses its power [18,19]. The rotation matrix C is defined by $C = (e_4^2 - e_v^T e_v) I_3 + 2 e_v e_v^T - 2 e_4 e_v^{\times}$ where $\|C\| = 1$ and $\dot{C} = -\omega_e^{\times} C$ [8]. The error quaternion (e_v, e_4) satisfies $e_v^T e_v + e_4^2 = 1$.

We assume that exact attitude and velocity measurements are available and each actuator has a known maximum torque $u_{\tau i,max}$ satisfying

$$|u_{\tau i,\max}| > J_M\left(c_1^2 + c_2\right) + l_g. \tag{11}$$

In this paper, the objective is to develop an adaptive hybrid fault-tolerant control law u subject to actuator constraints given by (11) to guarantee that the attitude tracking errors converge to the equilibrium point asymptotically without the unwinding phenomenon, which means $(0,0,0,\pm 1)^T$ is global stability for the rigid spacecraft in the presence of the actuator fault described by (8) and (9).

$$|u_{\tau i}| \le u_{\tau i,\max}. \tag{12}$$

3. Control Design

3.1. Hybrid System

Motivated by the work in [25,29], the following hysteresis-based hybrid function is introduced firstly to avoid the unwinding phenomenon.

$$\hbar \begin{cases} \dot{x} = \mathrm{M}(x), & x \in D, \\ x^+ = N(x), & x \in E. \end{cases} \tag{13}$$

where the flow map $\mathrm{M} : R^n \to R^n$ belongs to the flow set D, the jump map $N : R^n \to R^n$ belongs to the jump set E and x^+ represents the state value immediately after a jump [29].

Based on the hybrid system, we first introduce the following coordinate transformation S

$$S = \omega_e + h\gamma^2 e_v. \tag{14}$$

where γ denotes the update law defined in (20) and the auxiliary variable $h \in \hbar = \{-1, 1\}$ satisfies $h^+ = -h$. The continuous set D and the jump set E are defined, respectively, as follows.

$$D = \left\{x \in S^3 \times R^3 \times \hbar : \ he_4 > -\eta\right\}. \tag{15}$$

$$E = \left\{x \in S^3 \times R^3 \times \hbar : \ he_4 \leq -\eta\right\}. \tag{16}$$

where $x = \{q_e, \ \omega_e, \ h\}$, $\eta \in (0, 1)$ indicates the hysteresis gap.

Remark 1. *It is worth noting that h is chosen to change the desired rotation direction to push q_e to either $(0, 0, 0, 1)^T$ or $(0, 0, 0, -1)^T$. Thus, the desired rotation direction changes only when there is a significant benefit in switching it, where "significant" is defined precisely by the selection of η. The hysteresis width η manages a trade-off between robustness to disturbance and a small amount of hysteresis-induced inefficiency [25].*

3.2. Controller Formulation

The hybrid saturation and fault-tolerant attitude control (HSFC) is proposed as:

$$u = u_1 + u_2. \tag{17}$$

where

$$u_1 = -k\frac{S}{(|S_i| + \gamma^2\delta)} + (C\omega_d)^\times JC\omega_d + JC\dot{\omega}_d. \tag{18}$$

$$u_2 = -\left(\frac{1-\gamma_0}{\gamma_0}\|u_1\|\right)sign(\omega_e). \tag{19}$$

$$\dot{\gamma} = \frac{\alpha\gamma}{1 + 2\alpha k_1(1 - he_4)}\left(k\sum_{i=1}^{3}\left(\frac{he_{vi}\omega_{ei}}{(|S_i| + \gamma^2\delta)} - \frac{|\omega_{ei}|(1+\delta)}{|\omega_{ei}| + \gamma^2(1+\delta)}\right) - \frac{1}{2}k_1 he_v^T S\right). \tag{20}$$

where $sign(\cdot)$ denotes the sign function, k, k_1, α, δ are positive constants and $k > l_g$.

Remark 2. *It should be pointed out that the equilibrium point $(0, 0, 0, \pm 1)^T$ represents the same physical attitude for rigid spacecraft formulated by quaternion. When this double covering is neglected, the traditional controller can induce the notion called "unwinding", which leads to the spacecraft making an unnecessarily full rotation [25] and consuming more unnecessary energy. The proposed HSFC is designed to tackle the unwinding phenomenon.*

Utilizing the facts that $\|C\| = 1$, $\|e_4 I_3 + e_v^\times\| = 1$, $|e_i| \leq 1$ and $h^2 = 1$, the control torque u given by (17) can be upper bounded by

$$|u_{\tau i}| \leq \frac{1}{\gamma_0}\left(k + J_M\left(c_1^2 + c_2\right)\right), \quad u = [u_{\tau 1}, u_{\tau 2}, u_{\tau 3}]^T. \tag{21}$$

Rewriting Γu as $u_1 - (I_3 - \Gamma)u_1 + \Gamma u_2$ and utilizing the fact $\omega = \omega_e + C\omega_d$, we have

$$\begin{aligned} J\dot{\omega}_e = &-\omega_e^\times J\omega_e - \omega_e^\times JC\omega_d - (C\omega_d)^\times J\omega_e - (C\omega_d)^\times JC\omega_d \\ &+ J(\omega_e^\times C\omega_d - C\dot{\omega}_d) + u_1 - (I_3 - \Gamma)u_1 + \Gamma u_2 + d. \end{aligned} \tag{22}$$

4. Stability Analysis

Now, Theorem 1 of the main result of this paper is stated as follows.

Theorem 1. *Considering the rigid spacecraft described as (8) and (9), the developed approach defined by (17)–(19) ensures the attitude tracking errors globally converge to the equilibrium point asymptotically.*

Proof. The proof includes the following two consecutive main steps. First, when $x \in D$, all the states are continuous and h remains unchanged such that $\dot{h} = 0$; we prove that system states are stable in set D by using LaSalle's invariance principle for the hybrid system. Second, when $x \in E$, the jump only occurs with the variable h and the other system states are still continuous; we prove that system states are stable in set E.

Step 1. The following positive-definite Lyapunov function candidate is proposed.

$$V = \gamma^2 \frac{k_1}{2}\left[(1-he_4)^2 + e_v^T e_v\right] + \frac{1}{2}\omega_e^T J\omega_e + \frac{\gamma^2}{2\alpha}. \tag{23}$$

Note that the following equality holds with the fact $e_v^T e_v + e_4^2 = 1$.

$$(1-he_4)^2 + e_v^T e_v = 1 - 2he_4 + e_4^2 + e_v^T e_v = 2 - 2he_4 = 2(1-he_4). \tag{24}$$

In light of (24), we can rewrite (23) as

$$V = \gamma^2 k_1(1-he_4) + \frac{1}{2}\omega_e^T J\omega_e + \frac{\gamma^2}{2\alpha}. \tag{25}$$

The time derivative of V along (22) takes

$$\dot{V} = -\gamma^2 k_1 h\dot{e}_4 + \omega_e^T J\dot{\omega}_e + \dot{\gamma}\gamma\left(\frac{1}{\alpha} + 2k_1(1-he_4)\right). \tag{26}$$

By virtue of the fact $\dot{e}_4 = -\frac{1}{2}e_v^T\omega_e$, (26) can be further formulated as

$$\dot{V} = \frac{1}{2}\gamma^2 k_1 he_v^T\omega_e + \omega_e^T J\dot{\omega}_e + \dot{\gamma}\gamma\left(\frac{1}{\alpha} + 2k_1(1-he_4)\right). \tag{27}$$

When $x \in D$, substituting $J\dot{\omega}_e$ from (22) into (27), it follows that

$$\begin{aligned}\dot{V} = {} & \tfrac{1}{2}\gamma^2 k_1 he_v^T\omega_e + \dot{\gamma}\gamma\left(\tfrac{1}{\alpha} + 2k_1(1-he_4)\right) \\ & + \omega_e^T\begin{pmatrix} -\omega_e^\times J\omega_e - \omega_e^\times JC\omega_d - (C\omega_d)^\times J\omega_e - (C\omega_d)^\times JC\omega_d \\ +J(\omega_e^\times C\omega_d - C\dot{\omega}_d) + u_1 - (I_3-\Gamma)u_1 + \Gamma u_2 + d \end{pmatrix}.\end{aligned} \tag{28}$$

Using Properties 1 and 2, this yields

$$\begin{aligned} & \omega_e^T\omega_e^\times = 0, \\ & \omega_e^\times C\omega_d = -(C\omega_d)^\times\omega_e, \\ & \omega_e^T\left((C\omega_d)^\times J + J(C\omega_d)^\times\right)\omega_e = 0. \end{aligned} \tag{29}$$

Upon utilizing the above facts, Equation (28) yields

$$\begin{aligned}\dot{V} = {} & \tfrac{1}{2}\gamma^2 k_1 he_v^T\omega_e + \dot{\gamma}\gamma\left(\tfrac{1}{\alpha} + 2k_1(1-he_4)\right) \\ & + \omega_e^T\left(u_1 + d - (C\omega_d)^\times JC\omega_d - JC\dot{\omega}_d\right) + \omega_e^T(-(I_3-\Gamma)u_1 + \Gamma u_2).\end{aligned} \tag{30}$$

Upon substituting the controller (18) into (30) and applying the fact that $\omega_e = S - h\gamma^2 e_v$, we obtain

$$\begin{aligned}\dot{V} = {} & \tfrac{1}{2}\gamma^2 k_1 he_v^T(S - h\gamma^2 e_v) + \dot{\gamma}\gamma\left(\tfrac{1}{\alpha} + 2k_1(1-he_4)\right) \\ & + \omega_e^T d + \omega_e^T(-(I_3-\Gamma)u_1 + \Gamma u_2) - k\sum_{i=1}^{3}\tfrac{\omega_{ei}S_i}{(|S_i| + \gamma^2\delta)}.\end{aligned} \tag{31}$$

In light of (14), we can rewrite (31) as

$$\begin{aligned}\dot{V} &= \tfrac{1}{2}\gamma^2 k_1 h e_v^T\left(S - h\gamma^2 e_v\right) + \dot{\gamma}\gamma\left(\tfrac{1}{\alpha} + 2k_1(1 - he_4)\right) \\ &+\omega_e^T d + \omega_e^T(-(I_3 - \Gamma)u_1 + \Gamma u_2) - k\sum_{i=1}^{3}\tfrac{\omega_{ei}^2 + h\gamma^2 e_{vi}\omega_{ei}}{(|S_i| + \gamma^2\delta)}.\end{aligned} \tag{32}$$

By virtue of the triangle inequality, we have

$$\begin{aligned}&\sum_{i=1}^{3}\tfrac{\omega_{ei}^2}{(|S_i| + \gamma^2\delta)} = \sum_{i=1}^{3}\tfrac{\omega_{ei}^2}{\left(|\omega_{ei} + h\gamma^2 e_{vi}| + \gamma^2\delta\right)}, \\ &\sum_{i=1}^{3}\tfrac{\omega_{ei}^2}{\left(|\omega_{ei} + h\gamma^2 e_{vi}| + \gamma^2\delta\right)} \geq \sum_{i=1}^{3}\tfrac{\omega_{ei}^2}{(|\omega_{ei}| + \gamma^2(1+\delta))}, \\ &\sum_{i=1}^{3}\tfrac{\omega_{ei}^2}{(|\omega_{ei}| + \gamma^2(1+\delta))} = \sum_{i=1}^{3}\left(|\omega_{ei}| - \tfrac{|\omega_{ei}|\gamma^2(1+\delta)}{|\omega_{ei}| + \gamma^2(1+\delta)}\right).\end{aligned} \tag{33}$$

Upon applying (33) and the facts that $\sum_{i=1}^{3}|\omega_{ei}| \geq \|\omega_e\|$ and $\|d\| \leq l_g$ to (32), we obtain

$$\begin{aligned}\dot{V} &\leq \tfrac{1}{2}\gamma^2 k_1 h e_v^T\left(S - h\gamma^2 e_v\right) + \dot{\gamma}\gamma\left(\tfrac{1}{\alpha} + 2k_1(1 - he_4)\right) \\ &\quad+\omega_e^T d + \omega_e^T(-(I - \Gamma)u_1 + \Gamma u_2) \\ &\quad-k\sum_{i=1}^{3}\left(|\omega_{ei}| - \tfrac{|\omega_{ei}|\gamma^2(1+\delta)}{|\omega_{ei}| + \gamma^2(1+\delta)}\right) - k\sum_{i=1}^{3}\tfrac{h\gamma^2 e_{vi}\omega_{ei}}{(|S_i| + \gamma^2\delta)}.\end{aligned} \tag{34}$$

After substituting the update law (20) into (34), we obtain

$$\dot{V} \leq -\frac{1}{2}\gamma^4 k_1 h^2 e_v^T e_v + \|\omega_e\| l_g - k\|\omega_e\| + \omega_e^T(-(I_3 - \Gamma)u_1 + \Gamma u_2). \tag{35}$$

Recalling the facts that $\sum_{i=1}^{3}|\omega_{ei}| \geq \|\omega_e\|$, $\gamma_0 \leq \gamma_i$ and $\|I_3 - \Gamma\| = \lambda_M(I_3 - \Gamma) \leq 1 - \gamma_0$, we have

$$\begin{aligned}&\omega_e^T\Gamma u_2 = \omega_e^T\Gamma\left(-\left(\tfrac{1-\gamma_0}{\gamma_0}\|u_1\|\right)sign(\omega_e)\right) \leq -\lambda_{\min}(\Gamma)\left(\tfrac{1-\gamma_0}{\gamma_0}\|u_1\|\right)\sum_{i=1}^{3}|\omega_{ei}| \\ &\leq -\gamma_0\left(\tfrac{1-\gamma_0}{\gamma_0}\|u_1\|\right)\sum_{i=1}^{3}|\omega_{ei}| = -(1-\gamma_0)\|u_1\|\sum_{i=1}^{3}|\omega_{ei}| \\ &\leq -(1-\gamma_0)\|u_1\|\|\omega_e\|.\end{aligned} \tag{36}$$

Substituting (19) and (36) into (35) yields

$$\dot{V} \leq -c\|\omega_e\| - \frac{1}{2}\gamma^4 k_1 h^2 e_v^T e_v + \|\omega_e\|(1-\gamma_0)\|u_1\| - (1-\gamma_0)\|u_1\|\|\omega_e\|. \tag{37}$$

In light of $h^2 = 1$, (37) can be rewritten as

$$\dot{V} \leq -c\|\omega_e\| - \frac{1}{2}\gamma^4 k_1 e_v^T e_v. \tag{38}$$

where

$$c = k - l_g > 0. \tag{39}$$

When $x \in E$, the jump occurs in V and we have

$$V(x^+) - V(x) = 2\gamma^2 k_1 h e_4. \tag{40}$$

In view of (16), we obtain

$$V(x^+) - V(x) \leq -2\gamma^2 k_1 \eta < 0. \tag{41}$$

It is clear from (38) that $\dot{V} \leq 0$ where $c > 0$, $\gamma^4 > 0$ and $k_1 > 0$, when $x \in D$. Moreover, $\dot{V} = 0$ implies that $e_v = 0$ and $\omega_e(t) = 0$. Otherwise, when $x \in E$, we can conclude that $\dot{V} \leq 0$ from (41). Hence, by applying LaSalle's invariance theorem [34] and theorem 7.6 from [35], we can conclude that $\lim_{t\to\infty} e_v(t) = 0$ and $\lim_{t\to\infty} \omega_e(t) = 0$.

Step 2. When $x \in E$, no jump occurs. Thus, we have

$$V(x^+) - V(x) = 0. \tag{42}$$

Actually, the set $\{x \in E : \ V(x^+) - V(x) = 0\}$ is empty. Using Theorem 4.7 in [35], the tracking errors converge to the largest invariant set $\Psi = \left\{ (\omega_e, q_e, h) \middle| \ \dot{V} = 0, \ he_4 \geq -\eta \right\}$. By virtue of (38), it is clear that $\dot{V} = 0$ means that $e_v = 0$ and $\omega_e(t) = 0$. □

Remark 3. *Comparing with our recent work in [5,32,33], the proposed control not only can guarantee the control torque of the actuator can be upper bounded a priori by selecting the controller parameters but also can compensate the partial failure of the actuator. This is in contrast to the work of [29,30] who only tackle the attitude tracking problem for the fault-free spacecraft system.*

Remark 4. *The saturation vector $W(\omega_e) = [w(\omega_{e_1}), w(\omega_{e_2}), w(\omega_{e_3})]^T$ is used to eliminate chattering caused by the discontinuous vector function $sign(\omega_e)$ in controller (19) and $w(\omega_{e_i})$ is given by*

$$w(\omega_{e_i}) = \begin{cases} \frac{\omega_{e_i}}{|\omega_{e_i}|} & |\omega_{e_i}| > \bar{\varepsilon}, \\ \\ \frac{\omega_{e_i}}{\bar{\varepsilon}} & |\omega_{e_i}| \leq \bar{\varepsilon}\,. \end{cases} \tag{43}$$

where $\bar{\varepsilon}$ is a small positive constant.

Remark 5. *To avoid control torque over the real actuator maximum output (that is actuator saturation) in advance, the parameters k and γ_0 are chosen to constrain the control amplitude, and k and γ_0 satisfy $k > l_g$ and $\gamma_0 \leq \gamma_i(t) \leq 1$, respectively. Moreover, γ_0 in Equation (19) is designed to compensate the partial loss of actuator effectiveness faults. For a healthy actuator, γ_0 is chosen as $\gamma_0 = 1$, while γ_0 is selected as $\gamma_0 \leq \gamma_i(t) \leq 1$ for the actuator partial loss effectiveness to compensate the fault. Finally, to avoid the unwinding phenomenon, $h = \{1, -1\}$ is chosen to change the desired rotation direction to push q_e to either $(0,0,0,1)^T$ or $(0,0,0,-1)^T$. In addition, a large value of $0 < \delta < 1$ will decrease the convergence rate.*

5. Simulation

The simulations are performed on the spacecraft used in [2] to illustrate the effectiveness and the improved performance of the proposed HSFC. It should be pointed out that the parameters used in the simulation except actuator failure are completely the same as [2]. The inertia matrix is $J = [22\ 1.2\ 0.9; 1.2\ 19\ 1.4; 0.9\ 1.4\ 18]\ \ \mathrm{kg} \cdot \mathrm{m}^2$. The desired angular velocity is selected as $\omega_d(t) = 0.05\ [\sin(\pi t/100),\ \sin(2\pi t/100),\ \sin(3\pi t/100)]\ \mathrm{rad/sec}$, the desired attitude is generated by (7) and the initial desired attitude is chosen as $q_d(0) = [0,\ 0,\ 0,\ 1]^T$. The initial update law is chosen as $\gamma(0) = 2.5$. The initial attitude and angular velocity of the spacecraft are $q(0) = [0.3,\ -0.2,\ -0.3,\ 0.8832]^T$ and $\omega(0) = [0.06,\ -0.04,\ 0.05]^T \mathrm{rad/sec}$, respectively. The external disturbance is chosen as $d(t) = [0.1\sin(t),\ 0.2\sin(1.2t),\ 0.3\sin(1.5t)]\ \mathrm{N} \cdot \mathrm{m}$.

In light of the above system parameters and utilizing Assumptions 1–3, we obtain

$$J_M = 22.8\ \mathrm{kg} \cdot \mathrm{m}^2,\ \ l_g = 0.3\ \mathrm{N} \cdot \mathrm{m},\ \ c_1 = 5 \times 10^{-2}\ ,\ \ c_2 = 4.71 \times 10^{-3}. \tag{44}$$

5.1. Verification of the Effectiveness of HSFC with Fault Compensation

The comparison is performed on both HSFC and HSFC without fault compensation term u_2 for the actuator faulted spacecraft to verify the fault-tolerant property of the proposed HSFC. It is assumed that the actuator failure matrix is chosen as $\Gamma = diag(0.5 +$

$0.01\sin(10t),\ 0.5+0.02\cos(20t),\ 0.5+0.03\sin(30t))$ and $\gamma_0 = 0.2$. The other parameters of the proposed HSFC are chosen as $k = 5$, $k_1 = 5$, $k_2 = 5$, $\alpha = 0.01$, $\bar{\varepsilon} = 0.005$ and $\delta = 0.05$.

The maximum torque of the actuator in practical system is assumed to be $|u_{\tau i,\max}| = 10\ \mathrm{N}\cdot\mathrm{m}$. According to Equations (21) and (44), the upper bound of the control torque is $8.6\ \mathrm{N}\cdot\mathrm{m}$ and satisfies $|u_{\tau i}| \leq 8.6\ \mathrm{N}\cdot\mathrm{m} \leq |u_{\tau i,\max}| = 10\ \mathrm{N}\cdot\mathrm{m}$, which means that the proposed HSFC can be an anti-saturated controller, due to the maximum actual control torque being constrained to $10\ \mathrm{N}\cdot\mathrm{m}$.

The simulation results of the HSFC without fault compensation term u_2 for the actuator faulted spacecraft are shown in Figures 1–3, while those of the HSFC with fault compensation term u_2 are illustrated in Figures 4–6. Clearly, the HSFC with fault compensation term u_2 converges to the equilibrium point fast due to the fault-tolerant property, as we see in Figures 4 and 5, while the HSFC without the fault compensation term u_2 takes more time to complete its tracking, as we see in Figures 1 and 2.

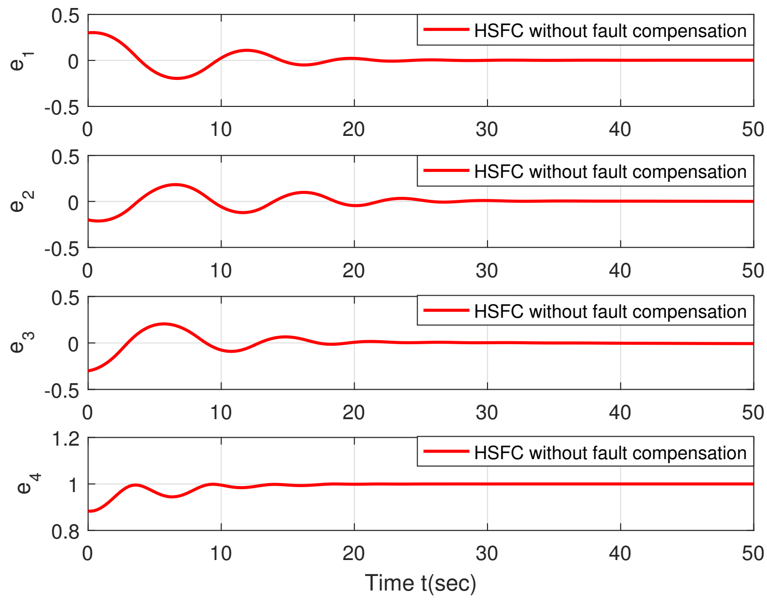

Figure 1. Attitude tracking errors.

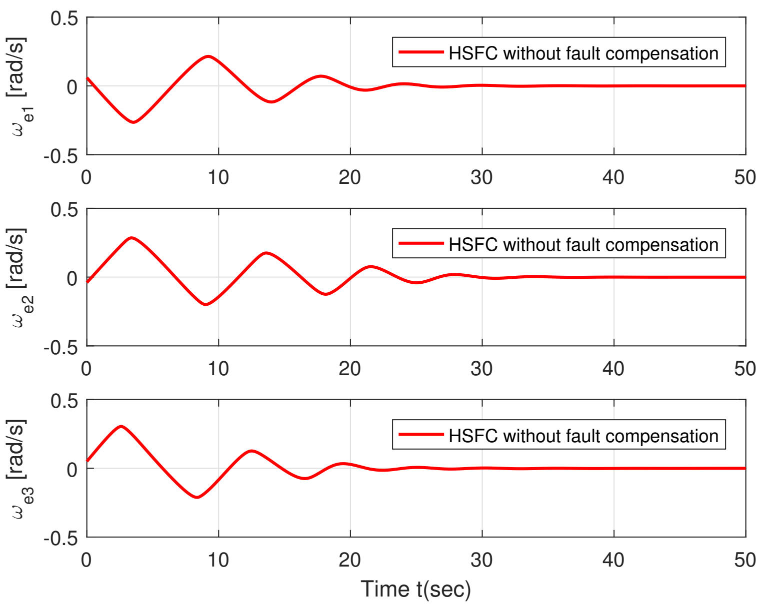

Figure 2. Angular velocity tracking errors.

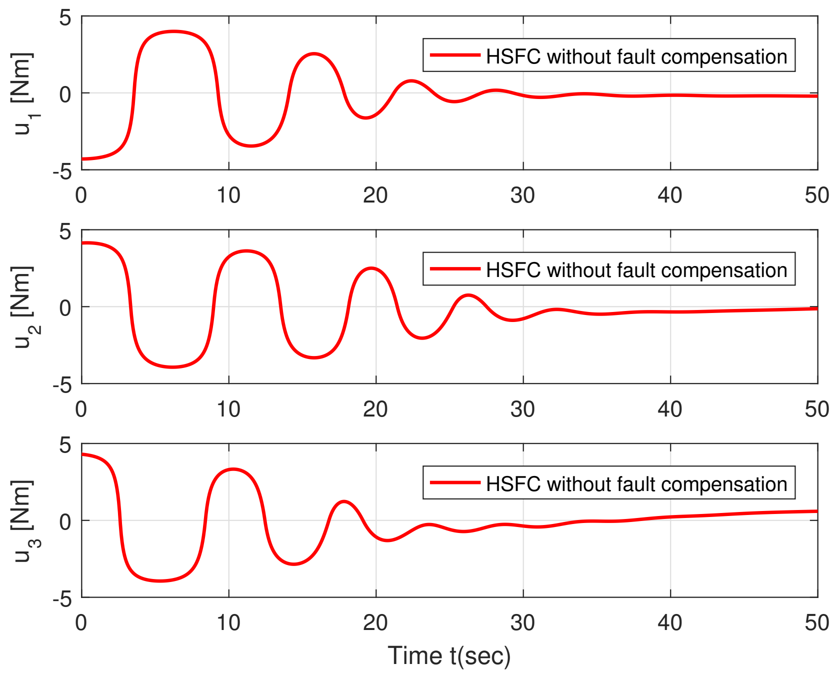

Figure 3. Control torque.

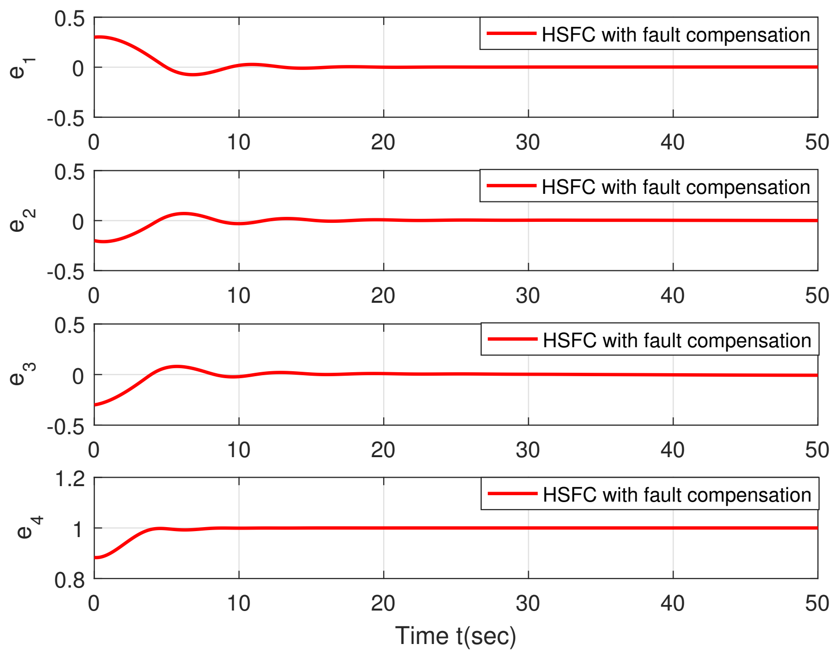

Figure 4. Attitude tracking errors.

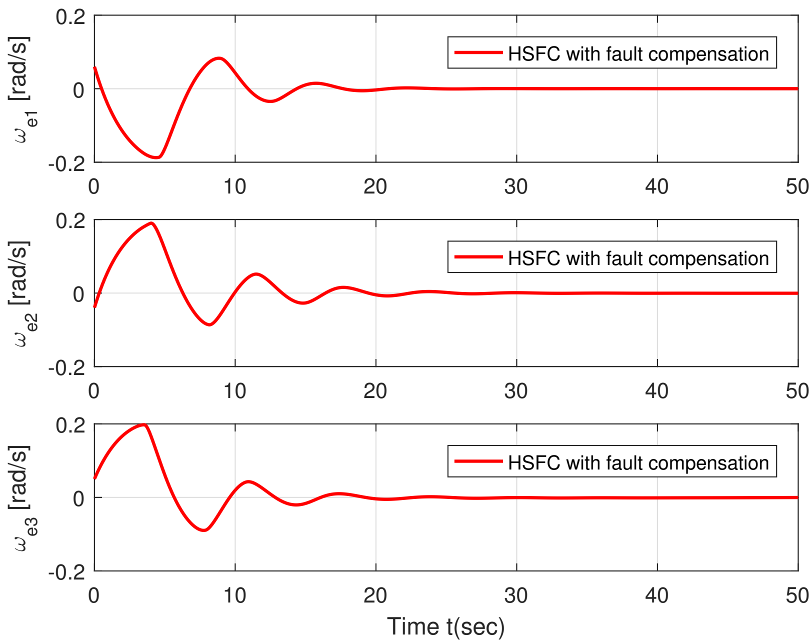

Figure 5. Angular velocity tracking errors.

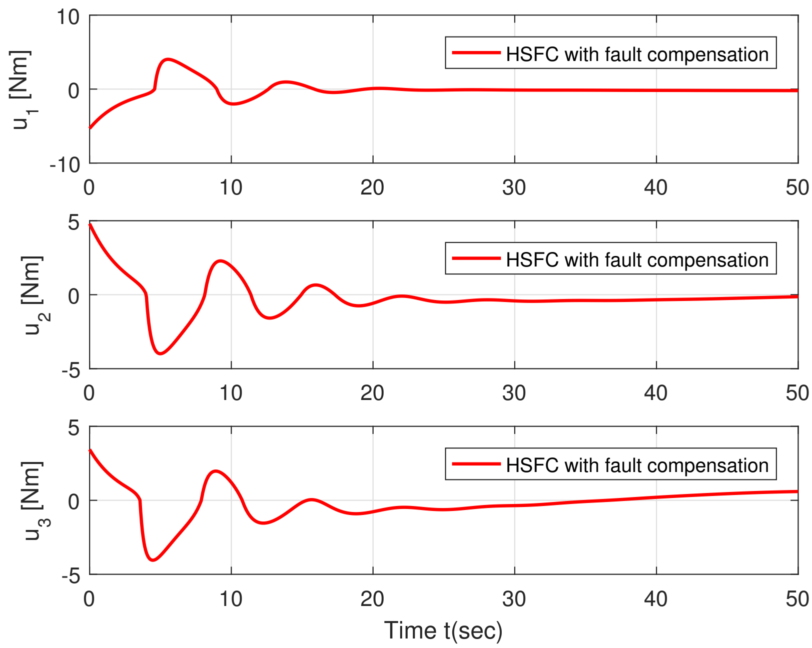

Figure 6. Control torque.

5.2. Comparisons with the AFNTSMC and SHOPD+

Firstly, a comparison with the AFNTSMC in [2] is performed to show the anti-unwinding performance of the proposed HSFC. Because the AFNTSMC does not consider actuator failure, the comparison is conducted on the fault-free spacecraft. Thus, the matrix $\Gamma = diag(1.0,\ 1.0,\ 1.0)$ is chosen to describe the healthy actuator and $\gamma_0 = 1$. The AFNTSMC is formulated as follows.

$$u = -\Big(\tau + u_{adp}(t)\Big)S(t) - \beta_0 sig^{\chi_0}(S). \tag{45}$$

$$S = \omega_e + \bar{k}_2 e_v + \bar{k}_3 S_{au}. \tag{46}$$

$$S_{aui} = \begin{cases} e_i^{\nu}, & \text{if } \bar{S}_i = 0 \text{ or } \bar{S}_i \neq 0,\ |e_i| \geq \varepsilon, \\ \iota_1 e_i + \iota_2 sign(e_i) e_i^2, & \text{if } \bar{S}_i \neq 0,\ |e_i| < \varepsilon. \end{cases} \tag{47}$$

and $\iota_1 = (2-\nu)\varepsilon^{\nu-1}$, $\iota_2 = (\nu-1)\varepsilon^{\nu-2}$.

$$\bar{S}_i = \omega_{ei} + \bar{k}_2 e_i + \bar{k}_3 e_i^{\nu}. \tag{48}$$

$$u_{adp} = diag(\hat{\chi}_i). \tag{49}$$

$$\hat{\chi}_i = \frac{1}{2}\varepsilon_{5i}^{-2}\hat{\psi}_i + \frac{1}{2}\varepsilon_{6i}^{-2}\hat{\phi}_i \|\xi\|^2. \tag{50}$$

$$\dot{\hat{\psi}}_i(t) = -\varepsilon_{3i}\hat{\psi}_i(t) + \frac{1}{2}n_{1i}\varepsilon_{5i}^{-2}|S_i(t)|^2. \tag{51}$$

$$\dot{\hat{\phi}}_i(t) = -\varepsilon_{4i}\hat{\phi}_i(t) + \frac{1}{2}n_{2i}\varepsilon_{6i}^{-2}|S_i(t)|^2\|\xi\|^2. \tag{52}$$

where τ and β_0 are diagonal constant matrices, and τ_i, β_{0i}, $i = 1,2,3$, k_2 and k_3 are positive constants, ε is a small positive constant, $0 < \chi_0 < 1$, ν_1, ν_2 are positive odd integers and satisfy $0 < \nu = \frac{\nu_1}{\nu_2} < 1$, and $\|\xi\| = \max\left\{\|\omega\|^2,\ \|\omega\|\right\}$.

The initial conditions are changed to $q(0) = [0.3,\ -0.2,\ -0.3,\ -0.8832]^T$ and $\omega(0) = [0.06,\ -0.04,\ 0.05]^T$rad/sec to verify the anti-unwinding performance. The following parameters of the AFNTSMC are chosen the same as [2]: $\varepsilon_{3i} = \varepsilon_{4i} = 0.35$, $\varepsilon_{5i} = \varepsilon_{6i} = 0.16$, $\bar{k}_2 = \bar{k}_3 = 1$, $\chi_0 = 0.5$, $\varepsilon = 0.001$, $\tau_i = 20$, $\nu_2 = 5$, $\nu_1 = 3$, $n_{1i} = n_{2i} = 6$, $\beta_{0i} = 10$ and $\hat{\psi}_i(0) = \hat{\phi}_i(0) = 0.1$. The parameters of the proposed HSFC are selected as $k = 5$, $k_1 = 5$, $k_2 = 5$, $\alpha = 0.1$, $\bar{\varepsilon} = 0.005$ and $\delta = 0.01$.

The comparison results are shown in Figures 7–10. From the comparison of Figure 7, it is clearly seen that the proposed HSFC can guarantee the attitude tracking errors converge to the equilibrium point $(0,0,0,-1)$ instead of $(0,0,0,1)$, which means that the unwinding phenomenon is tackled in comparison with the AFNTSMC. It is important to note that the unwinding property of the proposed HSFC has the benefit of decreasing excessive energy consumption compared to AFNTSMC, as we see in Figure 10.

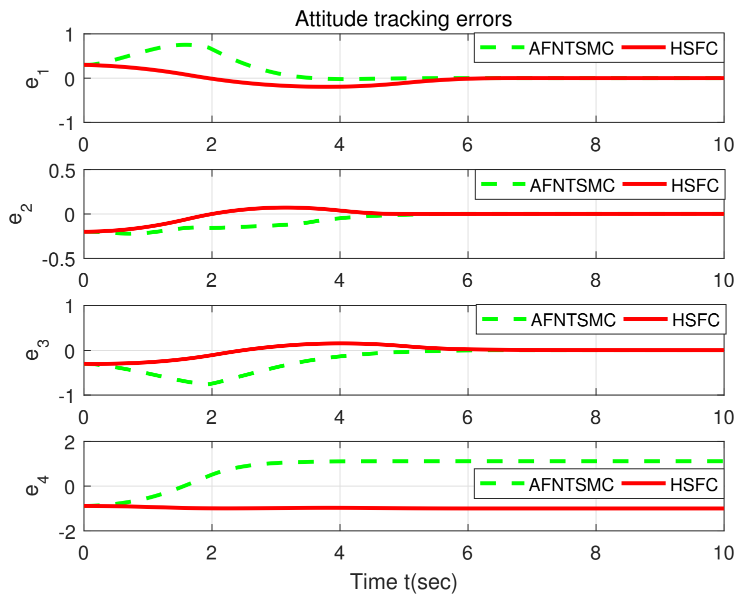

Figure 7. Comparison of attitude tracking errors.

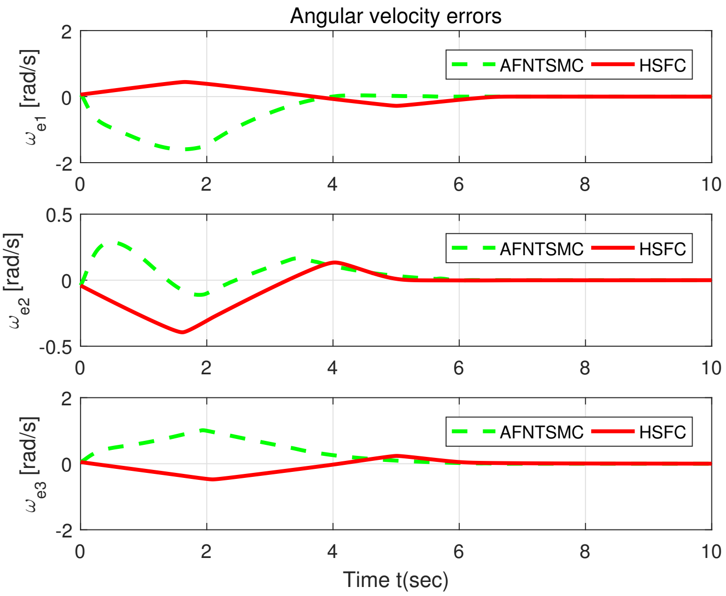

Figure 8. Comparison of angular velocity tracking errors.

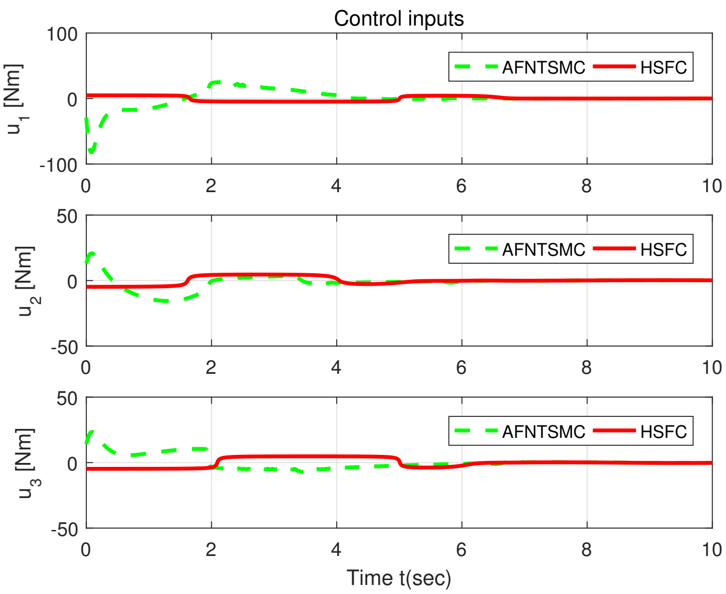

Figure 9. Comparison of control torque.

Secondly, a comparison with SHOPD+ in [29] is also illustrated to show the improved performance of the proposed HSFC. Both HSFC and SHOPD+ are anti-unwinding controllers. The SHOPD+ is given as follows

$$u = -k_4 h e_v - k_5 \left(e_4 I_3 + e_v^{\times}\right)^T S_a + (C\omega_d)^{\times} JC\omega_d + JC\dot{\omega}_d, \tag{53}$$

$$S_a(\nu_i) = \begin{cases} sign(\nu_i), & |\nu_i| \geq 1 \\ \nu_i, & |\nu_i| < 1 \end{cases}, \tag{54}$$

$$\begin{cases} \nu = q_c + B e_v \\ \dot{q}_c = -A\nu \end{cases}. \tag{55}$$

The parameters of the SHOPD+ are selected as: $k_4 = 30$ and $k_5 = 8$, $A = diag(1,1,1)$ and $B = diag(3,3,3)$.

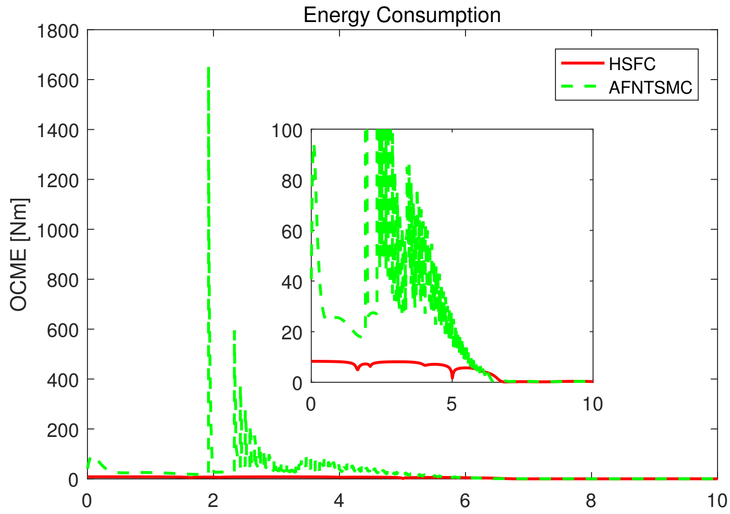

Figure 10. Comparison of energy consumption.

The comparison results are demonstrated in Figures 11–13. Obviously, HSFC and SHOPD+ can completely track their desired attitude and angular velocity within the allowable torques. Compared with SHOPD+, the proposed HSFC can achieve a fast transient over the SHOPD+ due to the fault compensation ability of HSFC, as we see in Figures 11 and 12. Moreover, the proposed HSFC has the benefit of decreasing excessive control torque compared to SHOPD+, as we see in Figure 13.

Based on the above simulation results, one can conclude that the designed HSFC can tackle the actuator saturation and partial loss failure problem of rigid spacecraft subject to external disturbances. Furthermore, in contrast to AFNTSMC in [2], the proposed HSFC also can overcome the unwinding phenomenon of rigid spacecraft. Compared with SHOPD+ in [29], the proposed HSFC can obtain a fast transient and compensate the actuator failure within the allowable torques of spacecraft.

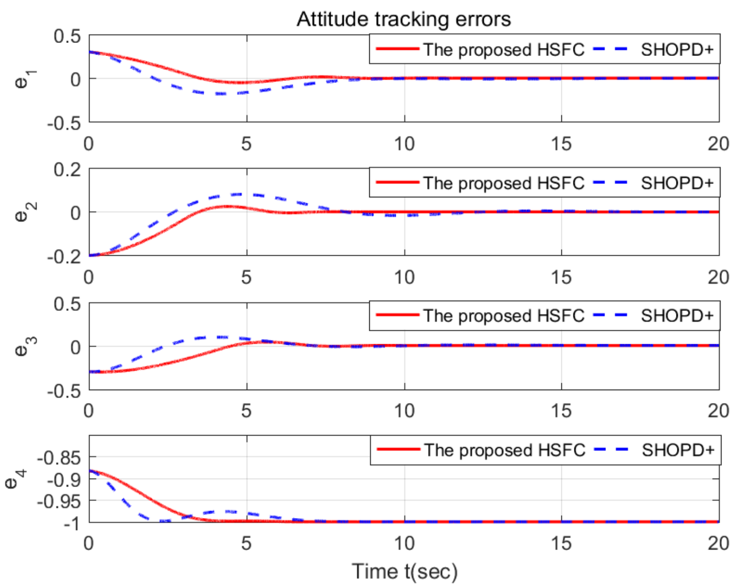

Figure 11. Comparison of attitude tracking errors.

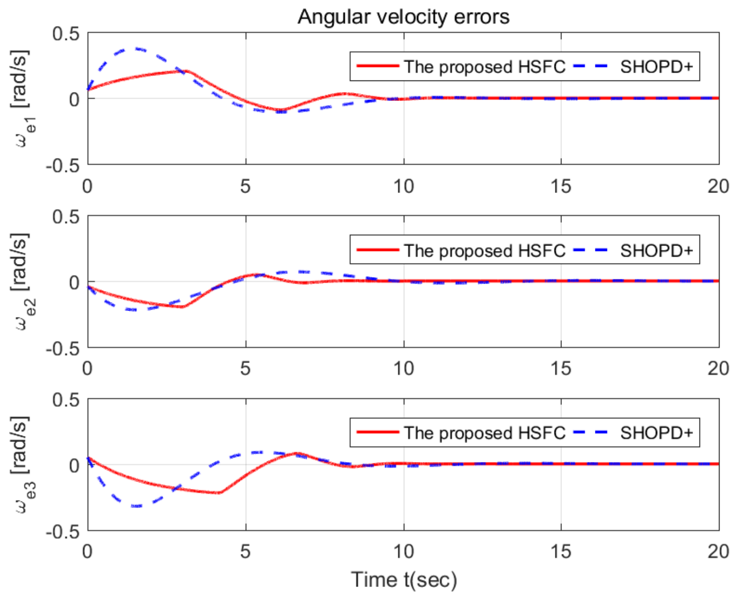

Figure 12. Comparison of angular velocity tracking errors.

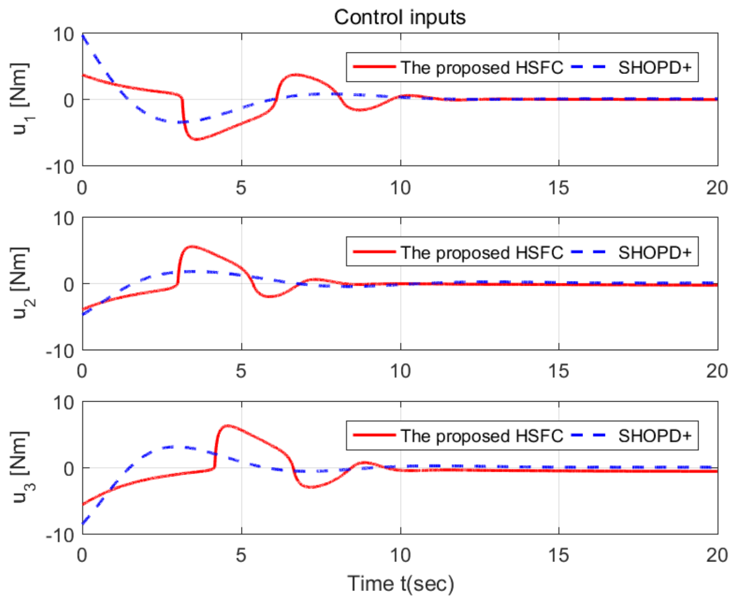

Figure 13. Comparison of control torque.

6. Conclusions

In this paper, a robust hybrid saturation and fault-tolerant control has been proposed for rigid spacecraft subject to external disturbances and actuator partial loss failure. The proposed HSFC can avoid actuator saturation and partial loss failure by selecting the control gains in advance, which implies that degraded performance of the actuator or unpredictable attitude tracking can be completely eliminated. Lyapunov's method is borrowed to prove the global asymptotic stability. The main features of the proposed HSFC include actuator saturation, fault-tolerance and robustness. Simulations verify the effectiveness and improved performance of the proposed control.

Author Contributions: Conceptualization, J.M. and Z.W.; methodology, Z.W.; software, Z.W.; validation, J.M., Z.W. and C.W.; formal analysis, C.W.; investigation, C.W.; resources, J.M.; data curation, J.M.; writing—original draft preparation, Z.W.; writing—review and editing, Z.W.; visualization, C.W.; supervision, C.W.; project administration, Z.W.; funding acquisition, Z.W. All authors have read and agreed to the published version of the manuscript.

Funding: This work was supported by the Education Department of Shaanxi Province with Grant/Award Numbers 21JK0675 and the Natural Science Foundation of Shaanxi Province with Grant/Award Numbers 2023-JC-QN-0738.

Institutional Review Board Statement: Not applicable.

Informed Consent Statement: Not applicable.

Data Availability Statement: The data that support the findings of this study are available from the corresponding author upon reasonable request.

Acknowledgments: The authors would like to thank the anonymous reviewers, Associate Editor and Editor for their valuable comments, which are helpful to improve the quality of this article.

Conflicts of Interest: The authors declare no conflict of interest.

References

1. Egeland, O.; Godhavn, J.M. Passivity-based adaptive attitude control of a rigid spacecraft. *IEEE Trans. Autom. Control* **1994**, *39*, 842–846. [CrossRef]
2. Lu, K.F.; Xia, Y.Q. Adaptive attitude tracking control for rigid spacecraft with finite-time convergence. *Automatica* **2013**, *49*, 3591–3599. [CrossRef]
3. Wang, Z.; Su, Y.X.; Zhang, L.Y. A new nonsingular terminal sliding mode control for rigid spacecraft attitude tracking. *J. Dyn. Syst. Meas. Control* **2018**, *140*, 051006. [CrossRef]
4. Wang, Z.; Su, Y.X.; Zhang, L.Y. Fixed-time attitude tracking control for rigid spacecraft. *IET Control Theory Appl.* **2020**, *14*, 790–799. [CrossRef]
5. Wang, Z.; Ma, J.; Hu, L.M. Predefined-time guaranteed performance attitude takeover control for non-cooperative spacecraft with uncertainties. *Int. J. Robust Nonlinear Control* **2023**, *33*, 7488–7509. [CrossRef]
6. Dixon, W.E. Adaptive regulation of amplitude limited robot manipulators with uncertain kinematics and dynamics. *IEEE Trans. Autom. Control* **2007**, *52*, 488–493. [CrossRef]
7. Perez-Arancibia, N.O.; Tsao, T.C.; Gibson, J.S. Saturation-induced instability and its avoidance in adaptive control of hard disk drives. *IEEE Trans. Control Syst. Technol* **2010**, *18*, 368–382. [CrossRef]
8. Boskovic, J.D.; li, S.M.; Mehra, R.K. Robust tracking control design for spacecraft under control input saturation. *J. Guid. Control Dyn.* **2004**, *27*, 627–633. [CrossRef]
9. Ali, I.; Radice, G.H.; Kim, J. Backstepping control design with actuator torque bound for spacecraft attitude maneuver. *J. Guid. Control Dyn.* **2010**, *33*, 254–259. [CrossRef]
10. de Ruiter, A.H.J.; Zheng, C.H. Adaptive spacecraft attitude tracking control with actuator saturation. *J. Guid. Control Dyn.* **2010**, *33*, 1692–1696. [CrossRef]
11. Su, Y.X.; Zheng, C.H. Globally asymptotic stabilization of spacecraft with simple saturated proportional-derivative control. *J. Guid. Control Dyn.* **2011**, *34*, 1932–1935. [CrossRef]
12. Su, Y.X.; Zheng, C.H. Velocity-free saturated PD controller for asymptotic stabilization of spacecraft. *Aerosp. Sci. Technol.* **2014**, *39*, 6–12. [CrossRef]
13. Su, Y.X.; Zheng, C.H. Unified saturated proportional derivative control framework for asymptotic stabilisation of spacecraft. *IET Control Theory Appl.* **2016**, *10*, 772–779. [CrossRef]
14. Su, Y.X.; Zheng, C.H. Single saturated PD control for asymptotic attitude stabilisation of spacecraft. *IET Control Theory Appl.* **2020**, *14*, 3338–3343. [CrossRef]
15. Xia, Y.Q.; Su, Y.X. Saturated output feedback control for finite-time attitude stabilization of spacecraft. *Proc. Inst. Mech. Eng. Part C J. Mech. Eng. Sci.* **2020**, *234*, 4557–4571. [CrossRef]
16. Yin, S.; Xiao, B.; Ding, S.X.; Zhou, D.H. A review on recent development of spacecraft attitude fault tolerant control system. *IEEE Trans. Ind. Electron.* **2016**, *63*, 3311–3320. [CrossRef]
17. Wang, Z.; Shan, J.J. Fixed-time consensus for uncertain multi-agent systems with actuator faults. *J. Frankl. Inst.* **2020**, *357*, 1199–1220. [CrossRef]
18. Cai, W.C.; Liao, X.H.; Song, D.Y. Indirect robust adaptive fault-tolerant control for attitude tracking of spacecraft. *J. Guid. Control Dyn.* **2008**, *31*, 1456–1463. [CrossRef]
19. Bustan, D.; Sani, S.H.; Pariz, N. Adaptive fault-tolerant spacecraft attitude control design with transient response control. *IEEE/ASME Trans. Mechatronics* **2014**, *19*, 1404–1411.
20. Shen, Q.; Wang, D.W.; Zhu, S.Q.; Poh, E.K. Inertia-free fault-tolerant spacecraft attitude tracking using control allocation. *Automatica* **2015**, *62*, 114–121. [CrossRef]
21. Wang, Z.; Su, Y.X.; Zhang, L.Y. Fixed-time fault-tolerant attitude tracking control for rigid spacecraft. *J. Dyn. Syst. Meas. Control* **2020**, *142*, 024502. [CrossRef]
22. Sun, R.; Shan, A.D.; Zhang, C.X.; Wu, J.; Jia, Q.X. Quantized fault-tolerant control for attitude stabilization with fixed-time disturbance observer. *J. Guid. Control Dyn.* **2021**, *44*, 449–455. [CrossRef]

23. Shen, Q.; Wang, D.W.; Zhu, S.Q.; Poh, E.K. Fault-tolerant optimal spacecraft attitude maneuver: An incremental model approach. *J. Guid. Control Dyn.* **2022**, *62*, 114–121.
24. Bhat, S.P.; Bernstein, D.S. A topological obstruction to continuous global stabilization of rotational motion and the unwinding phenomenon. *Syst. Control Lett.* **2012**, *61*, 595–601. [CrossRef]
25. Mayhew, C.G.; Sanfelice, R.G.; Teel, A.R. Quaternion-based hybrid control for robust global attitude tracking. *IEEE Trans. Autom. Control* **2011**, *56*, 2555–2566. [CrossRef]
26. Lee, T. Global Exponential Attitude Tracking Controls on SO(3). *IEEE Trans. Autom. Control* **2015**, *60*, 2837–2842. [CrossRef]
27. Schlanbusch, R.; Grotli, E.I. Hybrid certainty equivalence control of rigid bodies with quaternion measurements. *IEEE Trans. Autom. Control* **2015**, *60*, 2512–2517. [CrossRef]
28. Gui, H.C.; Vukovich, G. Global finite-time attitude tracking via quaternion feedback. *Syst. Control Lett.* **2016**, *97*, 176–183. [CrossRef]
29. Xia, Y.Q.; Su, Y.X. Saturated output feedback control for global asymptotic attitude tracking of spacecraft. *J. Guid. Control Dyn.* **2018**, *41*, 2300–2307. [CrossRef]
30. Xia, Y.Q.; Su, Y.X. Global saturated velocity-free finite-time control for attitude tracking of spacecraft. *IET Control Theory Appl.* **2019**, *13*, 1591–1602. [CrossRef]
31. Lee, D.; Leeghim, H. Reaction wheel fault-tolerant finite-time control for spacecraft attitude tracking without unwinding. *Int. J. Robust Nonlinear Control* **2020**, *30*, 3672–3691. [CrossRef]
32. Wang, Z.; Ma, J.; Wang, C. Predefined-time guaranteed performance attitude tracking control for uncertain rigid spacecraft. *IET Control Theory Appl.* **2022**, *16*, 1807–1819. [CrossRef]
33. Wang, Z.; Hu, L.M.; Ma, J. Distributed predefined-time attitude consensus control for multiple uncertain spacecraft formation flying. *IEEE Access* **2022**, *10*, 108848–108858. [CrossRef]
34. Slotine, J.J.E.; Li, W. *Applied Nonlinear Control*, 1st ed.; Prentice Hall: Englewood Cliffs, NJ, USA, 1991; pp. 41–126.
35. Sanfelice, R.G.; Goebel, R.; Teel, A.R. Invariance principles for hybrid systems with connections to detectability and asymptotic stability. *IEEE Trans. Autom. Control* **2007**, *52*, 2282–2297. [CrossRef]